

**High Saturation Magnetization, Low Coercivity and Fine YIG Nanoparticles Prepared by
Modifying Co-Precipitation Method**

S. Hosseinzadeh^a, M. Behboudnia^{*a}, L. Jamilpanah^b, M.H. Sheikhi^c, E. Mohajerani^d,
K. Tian^e, A. Tiwari^e, P. Elahi^f, S. M. Mohseni^{*b}

^aDepartment of Physics, Urmia University of Technology, Urmia, Iran

^bFaculty of Physics, Shahid Beheshti University, Evin, Tehran, 19839, Iran

^cDepartment of Communications and Electronics, School of Electrical and Computer
Engineering, Shiraz, Iran

^dLaser and Plasma Research Institute, Shahid Beheshti University, Evin, Tehran, 19839, Iran

^eDepartment of Materials Science and Engineering, University of Utah, Salt Lake City, UT
84112, USA

^fDepartment of Mechanical Engineering, University of Utah, Salt Lake City, UT, 84112, USA

*Corresponding author. E-mail Address: m-mohseni@sbu.ac.ir, majidmohseni@gmail.com (Seyed Majid Mohseni). mbehboudnia@gmail.com (Mahdi Behboudnia)

Abstract

Nanoparticles with their specific properties newly have drawn a great deal of attention of researchers [1-3] Yttrium iron Garnet magnetic nanoparticles (YIG-NPs) are promising materials with novel applications in microwave, spintronics, magnonics, and magneto-optical devices. However, achieving stable and remarkable magnetic YIG-NPs has been remaining as a great challenge. In this paper, synthesized YIG-NPs by modifying co-precipitation (MCP) method is reported. Structural and magnetic properties of final products are compared to those of the materials prepared by citrate-nitrate (CN) method. Smaller crystals and particle size have been found by MCP method comparing to that of synthesized by CN method. Using a relatively low annealing temperatures for both sets of samples (~ 700 °C), the final YIG samples prepared by MCP method show more structural purity than those made by CN method. Higher saturation magnetization (M_s) and lower coercivity (H_c) are observed in MCP YIG sample (23.23 emu/g and 30.1 Oe) than the CN prepared YIG sample (16.43 emu/g and 44.95 Oe). The Curie temperature is measured to be 569 °C for the MCP YIG sample determined from set of M_s measurement at different temperatures ranging from 80-600 K. These findings lead to significant improvement in quality of synthesized (synthetic methods) of YIG-NPs.

Keywords: YIG; Co-precipitation; Citrate-nitrate

1. Introduction

Nanoparticles with their specific properties newly have drawn great deal of attention of researchers Yittrium iron Garnet (YIG) with chemical composition $Y_3Fe_5O_{12}$ has been abundantly applied in magneto-optical and microwave devices, such as optical insulator, circulators, oscillators and phase shifters [4-6] owing to its narrow linewidth in magnetic resonance, high electrical resistivity, controllable saturation magnetization and large magneto-optical Faraday rotation [7, 8]. Physical responses of YIG specimen are strongly dependent on their microstructure. Moreover, thanks to rapid development in nanotechnology, YIG magnetic nanoparticles (YIG-NPs) have also been investigated variously based on their nanostructure properties [9-13]. Generally, YIG particles can be synthesized using various methods such as co-precipitation, solid-state procedure, auto-combustion and sol-gel methods [14-18]. These methods require high calcination temperature, which decreases monodispersity and also increases particle size. Moreover, the requirement of high heat treatments to prevent reaching any intermediate phases is the distinct disadvantage of these methods. Among above mentioned methods, sol-gel and co-precipitation methods, under some controlled synthesis conditions, have successfully been used for synthesis of nanoparticles. In each method, different parameters like pH, reaction time and temperature and concentration of the materials and solution play a significant role to achieve intended nanoparticles with desired size, shape, and structure [19]. Synthesis of YIG powder via citrate-nitrate (CN) technique, categorized in sol-gel methods, has drawn attentions due to significant advantages such as good mixing texture of precursors, excellent chemical homogeneity of the final products and lower synthesis temperatures compared to other methods [20, 21]. As a comprehensive study, Nguyet et al. [22] synthesized

YIG magnetic NPs by CN at pH=10 followed by annealing at 800 °C for 2h and reported magnetic field and temperature dependencies of magnetization of YIG powder with particle sizes ranging from 45-450 nm.

However, the most prevalent method for synthesizing magnetic NPs is the chemical co-precipitation technique [23-25]. There are several reports on synthesis of YIG magnetic NPs using chemical co-precipitation technique due to its main characteristic features such as simplicity and controllability of the process, low cost, high turnout [26, 27]. It appears likely that the synthesis of fine YIG-NPs at low processing temperatures still has plenty of room to delve in. Generally, NPs of relatively narrow size distributions can be synthesized by co-precipitation technique provided that a short nucleation takes place and be followed by a slower subsequent phase growth. The type of introduced salts, ratio of ions, temperature of the solution, pH, stirring speed and solvents type are the main parameters that must be precisely tuned to yield NPs of desired size with relatively narrow distribution. The purpose of gaining low particle size with high M_s and narrow size distribution has been the topic of many efforts done by authors. Rajendran et al. [28] reported YIG particles with average sizes of 9, 14, 25 nm which were synthesized by co-precipitation followed by modifying the product by chemical treatment. The sample with average particle size of 25 nm showed saturation magnetization (M_s) of 20.6 emu/g and no room temperature magnetic moment was reported for the particles having sizes of 9 and 14 nm. Godoi et al. [29, 30] carried out the synthesis of YIG powder by co-precipitation. He and his colleague obtained single phase YIG after annealing the precipitations at 1100 °C and the powder particles were of an average size of about 500 nm. Ristic et al. [31] obtained mainly YIG phase but with a small amount of $YFeO_3$ after annealing at 1200 °C and an ammonia solution in to the aqueous solution of Y- and Fe- nitrates up to pH~10.4. In a study by Rashad et al. [32], the

single phase YIG powder was obtained only after annealing the precipitations at 1200 °C via a NaOH solution route. Therefore, getting high saturation magnetization with small size particles and also phase purity of YIG at low temperature synthesis are the broken down purposes for researchers.

In present paper, we report on a low-temperature (700 °C) synthesis of small YIG magnetic NPs via a modifying co-precipitation (MCP) method using DMF as a primary solvent before and during precipitation. We then dissolved precipitation in the solution of citric acid which after washing the precipitates, act as fuel during annealing process. These two modifying approaches lead to formation of small single phase YIG magnetic NPs. We obtained small NPs (~17 nm) with narrower size distribution, higher saturation magnetization (23.23 emu/g) and lower coercivity (30.1 Oe) in comparison with others works. We have also synthesized YIG-NPs by the CN method in pH=1 at the same temperature used for our MCP method and comparing these two methods for final microstructure, size and magnetic properties. Our findings open pathways towards fine production of YIG magnetic NPs with controlled characteristics for distinctive applications.

2. Experimental

2.1 Materials

Ferric nitrate ($\text{Fe}(\text{NO}_3)_3 \cdot 9\text{H}_2\text{O}$), yttrium nitrate ($\text{Y}(\text{NO}_3)_3 \cdot 6\text{H}_2\text{O}$), citric acid, ethylene glycol, dimethylformamide (DMF) with 9.98% purity were purchased from Merck.

2.2 Preparation of the Samples

Two sets of YIG-NPs were prepared by CN and MCP methods. In CN synthesis, the solution was prepared by dissolving the Y and Fe nitrates in a stoichiometric ratio of Y: Fe = 3:5 in a de-

ionized water and a solution of citric acid was added to pH=1. The solution was heated at 80 °C and a gel was obtained after 2 hrs. This gel was dried at 110 °C and then heat treated for 36 h in ambient air at the temperature of 700 °C with a heating rate of 10 °C/min. The color of synthesized powder was brownish-green before heat treatment and turns chartreuse (green-yellow) after heat treatment. For synthesis of YIG-NPs by MCP, yttrium nitrate $Y(NO_3)_3 \cdot 6H_2O$ and iron nitrate $Fe(NO_3)_3 \cdot 9H_2O$ in 3:5 molar ratios were dissolved in DMF to form metal-organic solution. 4-5 drops of ethylene glycol were added as a complexing agent or as a polymerization agent [33, 34]. The solution was continuously stirred using a magnetic stirring bar and stirring speed of 4000 rpm. The mixed hydroxide $3Y(OH)_3 + 5Fe(OH)_3$ was co-precipitated from aqueous solutions up to pH ~ 10.5 by ammonium hydroxide and 25%-ammonia aqueous solution was used as precipitant. The precipitate was stirred for 30 min, centrifuged and then washed with deionized water ethanol. The precipitate was mixed with 2.5 g citric acid and 5.5 mL DI water to reach the pH=2 and continuously stirred at 60 °C to obtain solid precursor and finally heated to 700 °C for 2 hrs. The color of synthesized powder was olive.

2.3 Characterization of the samples

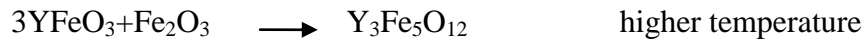
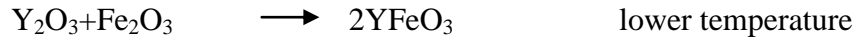
Thermal behavior of YIG precursors was determined by thermogravimetric analysis (TG) (model mettle Toledo C1600 analyzer) from ambient temperature to 850 °C in an air atmosphere with a heating rate of 10 °C/min. The crystalline structure of samples was characterized using X-ray diffractometer (STOE-STADI) with Cu $K\alpha$ ($\lambda = 0.154$ nm) radiation. For transmission electron microscopy (TEM) using (LEO 906, Zeiss, 100KV, Germany) and a high-resolution JEOL 2800 S/TEM system was used for performing transmission electron microscopy (HR-TEM). The sample was prepared as follows: a few prepared YIG-NPs were dispersed in absolute ethanol

ultra-sonication for 10 min and was dropped over carbon-coated copper grid and dried at room temperature. Room temperature magnetization measurement were done with vibrating sample magnetometer (VSM, Meghnatis Daghigh Kavir Co.) and temperature dependent magnetization measurements were done using a Microsense FCM-10 vibrating sample magnetometer (VSM), The volume-average diameter and size distribution of YIG magnetic NPs was measured by DLS (Shimadzu UV-1800 spectrophotometer). For DLS measurement, the YIG-NPs dispersed in absolute ethanol as a suitable solvent with appropriate dispersing agents and sonicate it for 10 min.

3. Results and discussion

3.1. X-Ray Diffraction (XRD) Study

Figure 1 shows XRD pattern of YIG for CN and MCP samples annealed at 700 °C at the room temperature. Prepared samples from CN contain YIG phase, along with peaks that can be attributed to maghemite ($\gamma\text{-Fe}_2\text{O}_3$), hematite ($\alpha\text{-Fe}_2\text{O}_3$) and orthoferrite (YFeO_3). These residual phases may be formed due to insufficient sintering time or temperature. The proposed crystallization process can be described by following reactions [35, 36]:



Prepared sample by MCP method (annealed at 700°C) completely contains YIG phase with very negligible contribution of intermediate phases. Therefore, crystallization occurs at lower temperature which can be happened because of using DMF as the solvent instead of water of precursors before precipitation process takes place. DMF as a polar solvent helps the diffusion and increases effective contact of the reactant molecules compared with water, which could well

disperse the ions and surround each ion during the precipitation process [37]. DMF as an organic solvent and citric acid as a complexing agent, helps to bring the yttrium and iron cations closer to each other. If the cations are close enough to each other, crystallization of oxide phase requires a much lower amount of energy in the system which will assist the formation of crystalline structure in lower temperature. Using Miller indices, the unit cell parameter was determined to be $a_0 = 12.404 \text{ \AA}$ which is larger than the bulk value of $a_0 = 12.3774 \text{ \AA}$ (JCPDS 33-693). Similarly, an increase in a_0 is observed for, $a_0 = 12.416 \text{ \AA}$. Crystal size was calculated by fitting of all the peaks and taking average of all the sizes obtained by Scherrer's equation. The average crystal size obtained from CN and MCP methods are 23 nm and 17 nm, respectively.

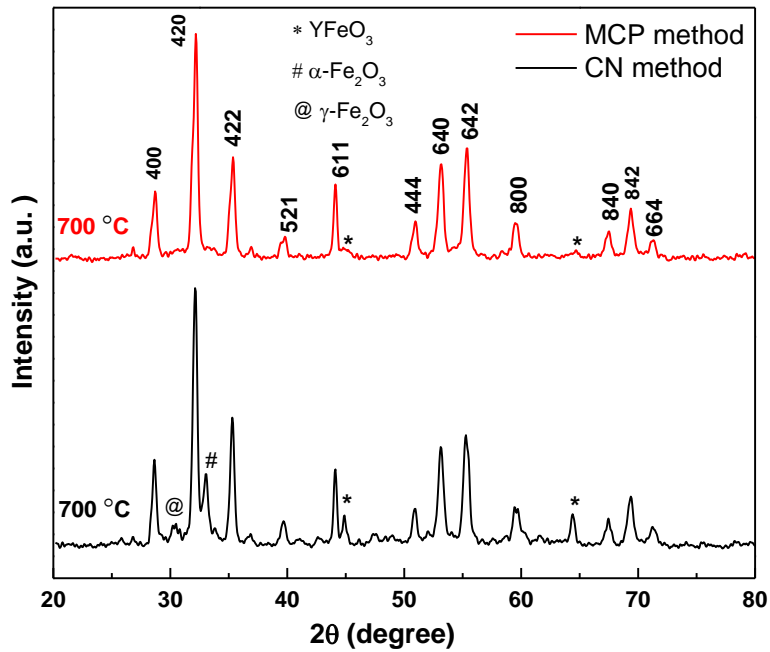


Figure 1: XRD pattern of (a) CN YIG-NPs and (b) MCP YIG-NPs at room temperature

3.2. Thermogravimetric Analysis (TGA)

As observed in XRD data, the sample prepared by MCP method is more crystalline and simultaneously has a lower crystal dimensions in comparison with the one prepared by CN method. In order to investigate the decomposition performance under air atmosphere, TGA technique is carried out for MCP prepared YIG sample. Figure 2 shows TGA curve of this sample and the steps of decomposition process in MCP method are shown. The TGA curve showed an overall weight loss of 58.6%. The weight loss of <10 % in the temperature range of 100-190 °C is due to evaporation of residual water molecules from the gels. The second weight loss which is about 63% of the overall weight loss occurs in the temperature range of 190-500 °C and can be considered as decomposition of remaining organics or oxidation of residual carbons. The weight loss in the temperature range of 500-690 °C is associated with crystallization of YFeO_3 and the last weight loss occurs at the temperature range of 690-760 °C which corresponds to formation and crystallization of YIG. It is granted that the starting temperature of decomposition is 190 °C and YIG formation completes between 690 to 760 °C. We noticed that the crystallization temperature is considerably decreased when organic acids are used. These molecules contain carbon which can act as fuel in the annealing process [16]. This means that higher local temperature assists the crystallization of compound. We used minimum amount of citric acid at 700 °C in MCP method to get smallest particle size. On the other hand, because of low annealing temperature we chose pH of 1 for the prepared sample by CN method among pH of 1, 2 and 3 reported in literatures in order to obtain complete phases of YIG since it is reported that by reducing pH, annealing temperature will decrease as well. The details of CN method and related TG curves can be found in referenced literature [14, 38].

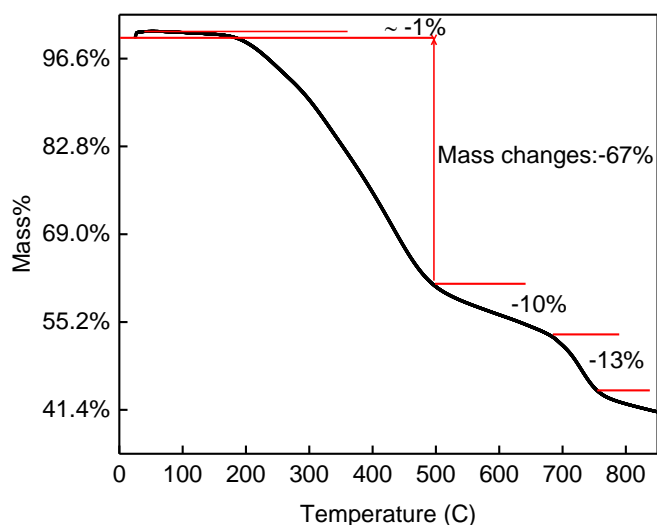


Figure 2: TGA curve of YIG particles prepared by MCP method.

3.3. Morphology and size of particles

Figure 3 shows TEM images of YIG-NPs prepared by CN and MCP methods. High resolution TEM (HRTEM) and SAED pattern for MCP YIG sample is presented in the figure 3a corresponds to YIG-NPs synthesized by CN method. It can be seen that particles are aggregated and exhibit irregular shapes without shaped borders. Figure 3b consequently determines that the size and line shape distribution of the particles. Because of the observed aggregation in TEM images of this sample the DLS results show a much larger size for it. Agglomeration of NPs in the absence of surfactants is common[39]. When we disperse magnetic nanoparticles in solution (ethanol) for DLS measurement, the magnetic interaction among the NPs larger than 20 nm in diameter is large enough to dominate the Brownian force among them while the smaller NPs remain stable in the solvent[1, 40]. Thus, considering the tendency of agglomeration of YIG NPs prepared by CN (their size are bigger than 20nm) in spherical aggregates the size was obtained by DLS is different by the size obtained by TEM and XRD. Figure 3c illustrates TEM

photograph of YIG-NPs synthesized by MCP method showing moderate clustering of particles and we can observe some small aggregations, which are composed of primary particles with the size distribution of 10-20 nm, matches the result of DLS measurement. Figure 3d describes in accordance with the calculated values for crystal size by the Scherrer's equation, the mean diameter of YIG-NPs prepared by MCP is 17 nm, which agrees with the values calculated from XRD. The YIG magnetic NPs prepared by MCP are nearly single crystal and the TEM analysis is quite consistent with the size distribution analyses mentioned above. The inset of Figure 3d shows the SAED pattern of YIG magnetic NPs synthesized by MCP, and annealed at 700 °C which contains single crystals. The bright spots are indexes to the (642), (422), (444), (644), (420), and (842) of the YIG-NPs. Figure 3e shows the lattice fringe image. The fringe spacing is measured to be 0.31 nm, 0.22 nm and 0.25 nm which correspond to the (400), (521) and (422) crystallographic plane of YIG and we show only the 0.22 nm space in the figure.

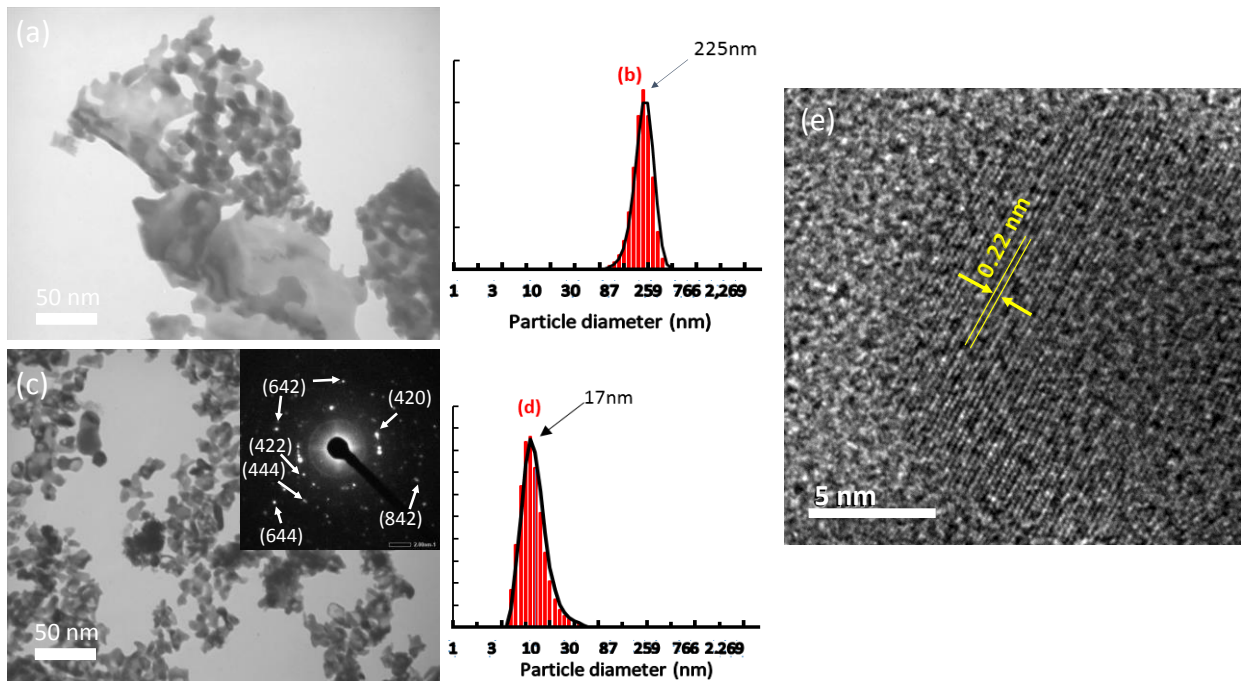


Figure 3: a) TEM image, b) size distribution from DLS of YIG-NPs synthesized by CN, c) TEM image, d) size distribution from DLS of YIG-NPs synthesized by MCP method, e) HRTEM of YIG-NPs synthesized by MCP method.

3.4. Magnetic Hysteresis Loops

In order to see the effect of synthesis method on the magnetic properties of YIG magnetic NPs, the magnetic response of the samples in the magnetic field was analyzed and evaluated by VSM at different temperatures. Figure 4 shows the hysteresis loops recorded at room temperature for both samples. The M_s of CN and MCP prepared samples are 16.43 and 23.23 emu/g, respectively. It is shown that YIG particles prepared by CN method have a lower value of M_s than those prepared by MCP method, which is more than the M_s reported in literatures [26, 28]. The lower measured value of magnetic saturation in CN method originated from existence of intermediate phases such as $\alpha/\gamma\text{-Fe}_2\text{O}_3$ which is a weak ferromagnetic compound and YFeO_3 which is antiferromagnetic compound [41, 42]. The presence of mentioned intermediate phases is owing to the insufficient annealing temperature which exacerbates YIG transition in CN method. Moreover, magnetic NPs synthesized by CN method have larger H_c and M_r than MCP prepared NPs (inset of Figure 4). We attribute this phenomenon to the existence of secondary phases and increment of magnetically disordered in structures [22, 43]. The data of H_c , M_s and M_r for both sets of samples can be seen in Table 1.

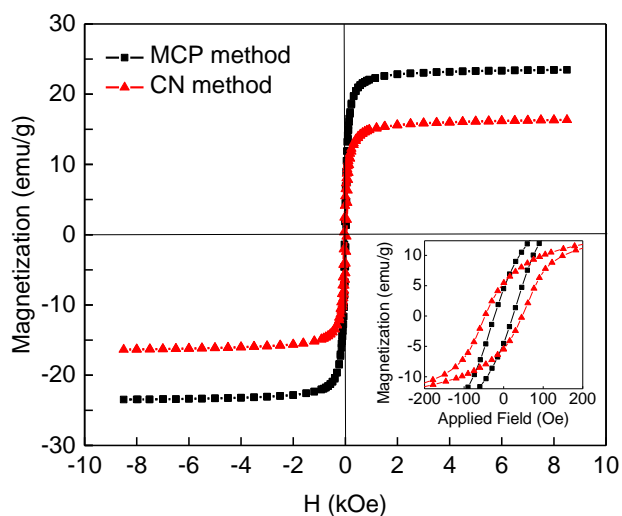


Figure 4: Magnetic hysteresis loops of YIG particles prepared by CN and MCP methods.

Table 1: Particle sizes obtained from XRD, TEM and DLS and M_s , H_c and M_r observed from VSM measurements.

Sample	Crystal size from XRD (nm)	Particle size from TEM (nm)	Particle size from DLS (nm)	M_s (emu/g)	H_c (Oe)	M_r (emu/g)
CN	23	> 20 nm	100-389	16.43	44.95	5.49
MCP	17	~20	6-26	23.23	30.1	4.52

To further study the magnetic properties of the YIG-NPs prepared via MCP method we measured temperature dependent M_s . The magnetization loops $M(H)$ in the temperatures ranging from 80 to 600 K were measured using VSM. The loops at 80, 100, 150, 200, 250 and 300 K are presented in Figure 5a and those ranging from 350 to 600K are presented in Figure 5b. A

common feature of the loops at different temperatures is the magnetization approaches to saturation above 2000 Oe. At 80 the M_s is $4.3 \mu_B/f.u.$, being 86% of theoretical value of YIG bulk which is $5 \mu_B/f.u$ [44]. Based on the relation $M_s^{experimental} = M_s^{bulk} [(D/2 - t)/D/2]^3$ for core-shell morphology where D is the particle diameter and t the surface layer thickness, a value of $t = 0.4$ nm is obtained according to mean particle size of 17 nm. At the inset of Figure 5a, it can be seen that the coercivity decreases as the temperature decreases. Also in the inset of the Figure 6 there is a phase change at temperatures higher than 500 K. At higher temperatures the coercivity vanishes which indicates a super paramagnetic behavior of the sample.

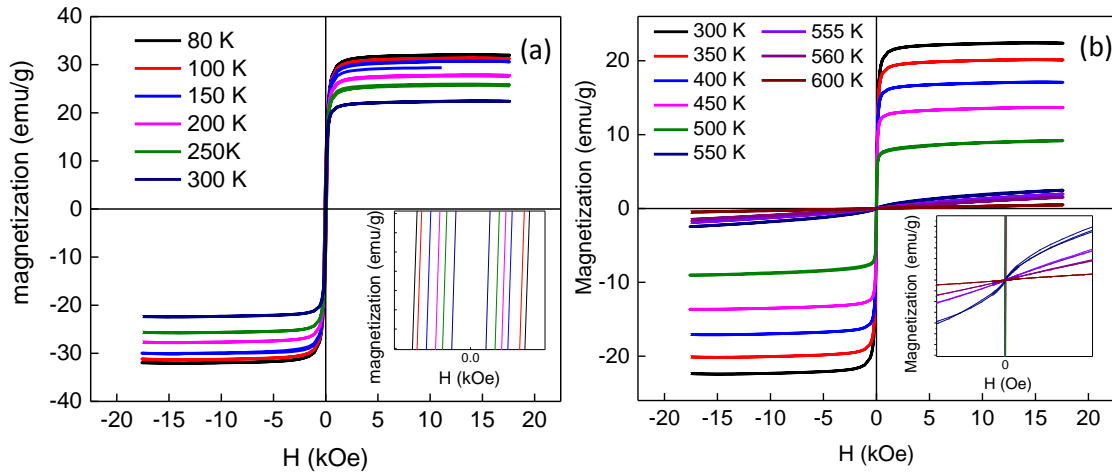


Figure 5: a) Hysteresis loops measured at 80, 100, 150, 200, 250 and 300 K for the MCP YIG-NPs. The inset shows the magnified region around the origin and b) Magnetization loops measured at temperatures between 350 and 560 K for the MCP YIG-NPs. The inset shows the magnified region around the origin.

The temperature dependence of the saturation magnetization for MCP YIG sample is exhibited in Figure 6. The experimental data was fitted using Bloch's equation:

$$M_T = M(0)[1 - (\frac{T}{T_0})^b]$$

Where, M_0 is the saturation magnetization at 0 K, T_0 is the temperature at which the M_s reduces to zero (Curie temperature, T_C) and the exponent b is the known Bloch's exponent. The fitted magnetic parameters are shown in the Figure 6. From this fit the Curie temperature of MCP YIG-NPs is found to be 569 K, not far from previous achievements (560 K) [1,2]. The Bloch exponent obtained to be 2.45 from the fitting process. In our samples, it is observed from the fitting parameters that the modified exponent (b) is larger than the exponent for bulk materials (3/2). For NPs, it is expected that as the size of the particle increases, b approaches to that of the bulk materials. The deviation from the original Bloch's law could be attributed to the surface effects and increment of the disordered states [6, 7]. In the case of our sample the particle size is small (17 nm) and this effect is expected to occur.

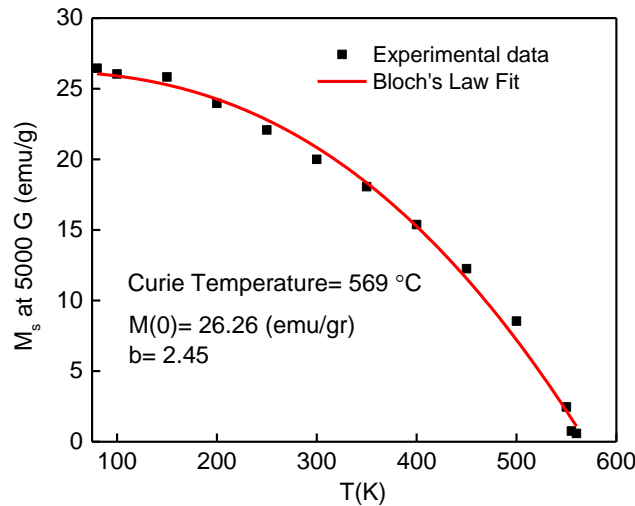


Figure 6: Saturation magnetization, M_s versus temperature, T for MCP sample. Solid line shows fitting with Bloch's equation.

Coercivity of the MCP sample at different temperatures is plotted in Figure 8. At approximately 300 K sample losses its coercivity. It is known from theoretical model that, for a given particle size, H_c decreases with increasing temperature following the Kneller's formula [22, 45]. In Kneller's formula H_c decreases by increasing temperature proportional to \sqrt{T} while it can be seen in Figure 8 that the reduction of H_c is nearly linear with T. Different particle sizes and different anisotropy alignments of particles can cause deviations from Kneller's formula but yet we see the procedure of reductive behavior in the figure.

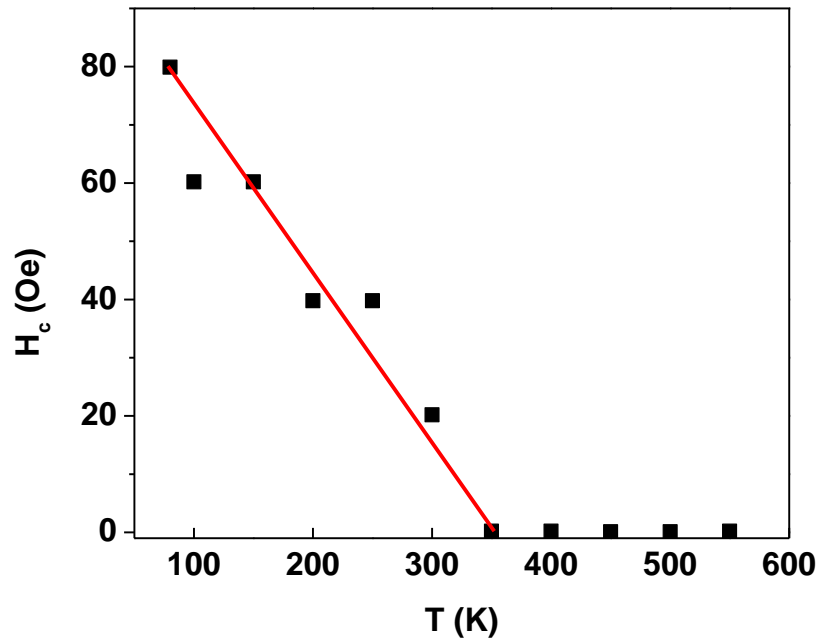


Figure 7: Coercivity, H_c versus temperature, T for MCP sample. Red line is a guide to eye and dots are experimental data

Conclusion

MCP method yielded to finer YIG-NPs with higher saturation magnetization and lower coercivity. Minimum amount of citric acid acts as a complexing agent and also as fuel in

annealing process in MCP method. Furthermore, citric acid takes a prominent role in decreasing crystallization temperature beside using DMF as polar solvent which both in their turns result in finer particles with relatively high saturation magnetization compared with the chemical CN method. YIG MCP particles show saturation magnetization of 23.23 emu/gr and the Curie temperature of 569 °C. The variation of saturation magnetization with temperature follows a $T^{2.4}$ power-law which is attributed to the small size of prepared YIG-NPs. Our findings can be used in synthesizing and achieving desired size and characteristics of YIG magnetic NPs.

Acknowledgments

S.M. Mohseni acknowledges support from Iran Science Elites Federation (ISEF), Iran Nanotechnology Initiative Council (INIC) and Iran's National Elites Foundation (INEF). A.T. wants to thanks US NSF for support through grant No. 1407650.

References

1. Khezri, S.H., A. Yazdani, and R. Khordad, *Pure iron nanoparticles prepared by electric arc discharge method in ethylene glycol*. The European Physical Journal-Applied Physics, 2012. **59**(3).
2. Khezri, S.H., et al., *Preparation of Pure Cobalt Nanoparticles by Electric Arc Discharge Method in Ethylene Glycol*. Modern Physics Letters B, 2013. **27**(09): p. 1350057.
3. Lu, A.H., E.e.L. Salabas, and F. Schüth, *Magnetic nanoparticles: synthesis, protection, functionalization, and application*. Angewandte Chemie International Edition, 2007. **46**(8): p. 1222-1244.
4. Kajiwara, Y., et al., *Transmission of electrical signals by spin-wave interconversion in a magnetic insulator*. Nature, 2010. **464**(7286): p. 262.
5. Uchida, K., et al., *Spin Seebeck insulator*. Nat Mater, 2010. **9**(11): p. 894-897.
6. Uchida, K.-i., et al., *Observation of longitudinal spin-Seebeck effect in magnetic insulators*. Applied Physics Letters, 2010. **97**(17): p. 172505.
7. Adam, J.D., et al., *Ferrite devices and materials*. IEEE Transactions on Microwave Theory and Techniques, 2002. **50**(3): p. 721-737.
8. Stancil, D. and A. Prabhakar, *Spin Waves: Theory and Applications, 2009*. Springer, New York.
9. Giri, J., et al., *Investigation on Tc tuned nano particles of magnetic oxides for hyperthermia applications*. Bio-medical materials and engineering, 2003. **13**(4): p. 387-399.

10. Grasset, F., et al., *Synthesis, magnetic properties, surface modification and cytotoxicity evaluation of $Y_3Fe_{5-x}Al_xO_{12}$ ($0 \leq x \leq 2$) garnet submicron particles for biomedical applications*. Journal of magnetism and magnetic materials, 2001. **234**(3): p. 409-418.
11. Serga, A., A. Chumak, and B. Hillebrands, *YIG magnonics*. Journal of Physics D: Applied Physics, 2010. **43**(26): p. 264002.
12. Bourhill, J., et al., *Ultrahigh cooperativity interactions between magnons and resonant photons in a YIG sphere*. Physical Review B, 2016. **93**(14): p. 144420.
13. Aldosary, M., et al., *Platinum/yttrium iron garnet inverted structures for spin current transport*. Applied Physics Letters, 2016. **108**(24): p. 242401.
14. Vaquero, P., M. Crosnier-Lopez, and M. Lopez-Quintela, *Synthesis and characterization of yttrium iron garnet nanoparticles*. Journal of solid state chemistry, 1996. **126**(2): p. 161-168.
15. Vaquero, P., M.A. López-Quintela, and J. Rivas, *Synthesis of yttrium iron garnet nanoparticles via coprecipitation in microemulsion*. Journal of Materials Chemistry, 1997. **7**(3): p. 501-504.
16. Vajargah, S.H., H.M. Hosseini, and Z. Nemati, *Preparation and characterization of yttrium iron garnet (YIG) nanocrystalline powders by auto-combustion of nitrate-citrate gel*. Journal of Alloys and Compounds, 2007. **430**(1): p. 339-343.
17. Vajargah, S.H., H.M. Hosseini, and Z. Nemati, *Synthesis of nanocrystalline yttrium iron garnets by sol-gel combustion process: The influence of pH of precursor solution*. Materials Science and Engineering: B, 2006. **129**(1): p. 211-215.
18. Akhtar, M.N., et al., *Impacts of Gd-Ce on the structural, morphological and magnetic properties of garnet nanocrystalline ferrites synthesized via sol-gel route*. Journal of Alloys and Compounds, 2016. **660**: p. 486-495.
19. Rajaeiyan, A. and M. Bagheri-Mohagheghi, *Comparison of sol-gel and co-precipitation methods on the structural properties and phase transformation of γ and α -Al₂O₃ nanoparticles*. Advances in Manufacturing, 2013. **1**(2): p. 176-182.
20. Vaquero, P. and M. Lopez-Quintela, *Influence of complexing agents and pH on yttrium-iron garnet synthesized by the sol-gel method*. Chemistry of Materials, 1997. **9**(12): p. 2836-2841.
21. Niyafar, M., et al., *Effect of indium addition on the structure and magnetic properties of YIG*. Journal of Magnetism and Magnetic Materials, 2010. **322**(7): p. 777-779.
22. Nguyet, D.T.T., et al., *Temperature-dependent magnetic properties of yttrium iron garnet nanoparticles prepared by citrate sol-gel*. Journal of Alloys and Compounds, 2012. **541**: p. 18-22.
23. Martínez-Mera, I., et al., *Synthesis of magnetite (Fe_3O_4) nanoparticles without surfactants at room temperature*. Materials Letters, 2007. **61**(23): p. 4447-4451.
24. Morrison, S.A., et al., *Atomic engineering of mixed ferrite and core-shell nanoparticles*. Journal of nanoscience and nanotechnology, 2005. **5**(9): p. 1323-1344.
25. van den Hoop, M. and J. Benegas, *Colloids and surfaces a: physicochemical and engineering aspects*. Colloids and Surfaces A: Physicochemical and Engineering Aspects, 2000. **170**(2-3): p. 151-160.
26. Kim, T. and M. Shima, *Reduced magnetization in magnetic oxide nanoparticles*. Journal of applied physics, 2007. **101**(9): p. 09M516.
27. Zhang, W., et al., *Low-temperature synthesis and microstructure-property study of single-phase yttrium iron garnet (YIG) nanocrystals via a rapid chemical coprecipitation*. Materials Chemistry and Physics, 2011. **125**(3): p. 646-651.
28. Rajendran, M., et al., *Size-dependent magnetic properties of nanocrystalline yttrium iron garnet powders*. Journal of Magnetism and Magnetic Materials, 2006. **301**(1): p. 212-219.
29. Godoi, R.H., et al., *Nanometric particles of yttrium ferrite*. Química Nova, 1999. **22**(6): p. 783-786.

30. Jafelicci, M. and R. Godoi, *Preparation and characterization of spherical yttrium iron garnet via coprecipitation*. Journal of magnetism and magnetic materials, 2001. **226**: p. 1421-1423.
31. Ristić, M., et al., *Influence of synthesis procedure on the YIG formation*. Materials letters, 2003. **57**(16): p. 2584-2590.
32. Rashad, M., et al., *Effect of synthesis conditions on the preparation of YIG powders via co-precipitation method*. Journal of Magnetism and Magnetic Materials, 2009. **321**(22): p. 3752-3757.
33. Leite, E., A. Maciel, and I. Weber, PNL Filho, E. Longo, COP Santos, AVC Andrae, CA Pakoscimas, Y. Manietle, WH Schreiner. Adv. Mater, 2002. **14**: p. 5.
34. Matsumoto, K., et al., *Preparation of bismuth-substituted yttrium iron garnet powders by the citrate gel process*. Journal of Applied Physics, 1991. **69**(8): p. 5918-5920.
35. Lee, H., et al., *Magnetic and FTIR studies of $\text{Bi}_x\text{Y}_{3-x}\text{Fe}_5\text{O}_{12}$ ($x=0, 1, 2$) powders prepared by the metal organic decomposition method*. Journal of Alloys and Compounds, 2011. **509**(39): p. 9434-9440.
36. Lee, H., et al., *Preparation of bismuth substituted yttrium iron garnet powder and thin film by the metal-organic decomposition method*. Journal of Crystal Growth, 2011. **329**(1): p. 27-32.
37. Derang Cao, H.L., et al., *High saturation magnetization of $\gamma\text{-Fe}_2\text{O}_3$ nano-particles by a facile one-step synthesis approach*. Scientific reports, 2016. **6**.
38. Galstyan, O., et al., *Magneto-optical visualization by Bi: YIG thin films prepared at low temperatures*. Journal of Applied Physics, 2015. **117**(16): p. 163914.
39. Khezri, S.H., A. Yazdani, and R. Khordad, *Effect of characteristics of media on cobalt and iron nanoparticles prepared by arc discharge method*. Journal of Industrial and Engineering Chemistry, 2014. **20**(2): p. 521-527.
40. Burke, N.A., H.D. Stöver, and F.P. Dawson, *Magnetic nanocomposites: preparation and characterization of polymer-coated iron nanoparticles*. Chemistry of materials, 2002. **14**(11): p. 4752-4761.
41. Mathur, S., et al., *Molecule Derived Synthesis of Nanocrystalline YFeO_3 and Investigations on Its Weak Ferromagnetic Behavior*. Chemistry of Materials, 2004. **16**(10): p. 1906-1913.
42. Marusak, L.A., R. Messier, and W.B. White, *Optical absorption spectrum of hematite, $\alpha\text{Fe}_2\text{O}_3$ near IR to UV*. Journal of Physics and Chemistry of Solids, 1980. **41**(9): p. 981-984.
43. Sanchez, R., et al., *Particle size effects on magnetic properties of yttrium iron garnets prepared by a sol-gel method*. Journal of magnetism and magnetic materials, 2002. **247**(1): p. 92-98.
44. Gilleo, M., *Superexchange interaction energy for $\text{Fe}^{3+}\text{-O}^{2-}\text{-Fe}^{3+}$ linkages*. Physical Review, 1958. **109**(3): p. 777.
45. Najmoddin, N., et al., *Effect of nanoconfinement on the formation, structural transition and magnetic behavior of mesoporous copper ferrite*. Journal of Alloys and Compounds, 2014. **598**: p. 191-197.

